Validation and inter-comparison of a novel Atmospheric Correction Method

Project number: AO10
Candidate number: 1046002
Supervisors: Dr R. Song and Professor R. G. Grainger

Abstract

The Sensor Invariant Atmospheric Correction (SIAC) module is a recently developed atmospheric correction module utilising a Bayesian framework to provide surface reflectance data from high resolution remote sensing measurements. Here, SIAC is applied to data acquired by the Sentinel-2 (S2) satellites, in order to investigate the accuracy of its atmospheric corrections over different landscapes, specifically forests, deserts, and urban areas. SIAC retrieved aerosol optical thickness (AOT) values are compared to ground measurements from Aerosol Robotic Network (AERONET) detectors. SIAC retrieved surface reflectance values are compared to S2-equivalent surface reflectance values derived from the Moderate Resolution Imaging Spectroradiometer (MODIS). SIAC AOT and surface reflectance retrieval performance is found to be encouraging, particularly with regards to surface reflectance. AOT retrievals are more effective in areas where the surface reflectance is lower, with results meeting target uncertainty thresholds for one forest detector (71.7 % of points within target uncertainties) and coming close for another forest detector (64.1 %). AOT retrieval accuracy is decreased over brighter areas with only 30.9 % and 45.2 % of points within the target limits for two desert detectors, and 25.0 % for an urban detector. However, this appears to be corrected in the surface reflectance retrieval with SIAC matching MODIS values to a reasonable degree of accuracy, with 50.0 % of points across three visible bands lying within target uncertainty limits for an area of forest, 59.5 % of points for an area of desert and most points matching seasonal trends in the reference data.

1 Introduction

Earth Observation (EO) satellites play a crucial role in monitoring the behaviour of Earth's atmosphere and surface. Each satellite is fitted with one or more instruments that make measurements of electromagnetic radiation as it orbits Earth. Observations of visible wavelengths are made to calculate the reflectance of Earth's surface, which is used widely including to calculate Earth's radiation budget (the balance of incoming and outgoing radiation), monitor crops to detect disease and water stress, and survey deforestation. In order to obtain accurate readings of Earth's surface, the interactions between the signal (in this case visible light) and the atmosphere need to be accounted for: the most significant effects are scattering and absorption by aerosols (any small solid particle suspended in the atmosphere) and water vapour [1]. 'Atmospheric correction' (AC) modules are used to derive the required reflectance data at Earth's surface (bottom-of-atmosphere, BOA) from the satellite measurements made at the top of the atmosphere (top-of-atmosphere, TOA). Typically, an AC module estimates the aerosol optical thickness (AOT, the additional optical path light travels through due to the presence of aerosols) and total columnar water vapour (TCWV, the amount of water that could precipitate out of a vertical column of the atmosphere) and uses these parameters as inputs in a radiative transfer model, which calculates BOA reflectance data from the predicted attenuation of the TOA signal. Variation in the estimated AOT has a significant impact on the output of the radiative transfer model, and so it is important for the AC module's AOT retrieval to be accurate [1]; this work is an evaluation of the performance of the AOT retrieval of the SIAC AC module. In all previous work investigating SIAC's AOT retrievals, no comparisons have been made between SIAC's effectiveness when applied to satellite observations across varying surface types, so this work analyses how SIAC AOT retrieval performance differs dependent on the surface cover and land use of the observed region.

SIAC is designed for use with the high resolution Sentinel-2 (S2) and Landsat-8 (L8) EO satellites. It uses well verified BOA surface reflectance data from MODIS, derived at a 500 m resolution in sinusoidal projection (a projection is a geometric mapping of Earth's surface into 2D, a sinusoidal projection preserves area but distorts shapes), and compares this to S2/L8 TOA data transformed to the same 500 m resolution sinusoidal projection. A 6S (Second Simulation of a Satellite Signal in the Solar Spectrum) radiative transfer model is used to convert the MODIS BOA data into TOA data to match the S2 data. SIAC updates the AOT and TCWV values used in the radiative transfer model to solve for an optimal estimate, then applies this to high resolution TOA S2/L8 data to retrieve high resolution BOA surface reflectance data. SIAC utilises Copernicus Atmosphere Monitoring Service (CAMS) aerosol values (at 40 km resolution) as priors in the minimisation problem. SIAC differs from other AC modules through its use of MODIS and CAMS datasets as priors, and its ability to give per-pixel uncertainty values through its Bayesian probabilistic framework. Furthermore, by applying an identical method to both S2 and L8 data, SIAC introduces the possibility of combining their results to provide greater temporal resolution of corrected observations.

Previous work demonstrates the good performance of SIAC AOT retrievals when ignoring variation across surface types [2], whilst comparisons have been made between the accuracy of retrievals from SIAC and other AC modules [3]. Previous work has also shown that the Sen2Cor AC module, which is currently widely used with S2 data, exhibits poor AOT retrieval results [4]; SIAC aims to provide more accurate atmospheric corrections for S2 data. This work is an in-depth investigation of SIAC's AOT retrieval performance across varied surface types; the approach is to compare SIAC retrieved AOT values with measurements made a ground level by AERONET detectors. Preliminary results are also obtained comparing SIAC retrieved surface reflectance values with equivalent MODIS retrievals. The data used in these analyses are introduced in Section 2, whilst Section 3 describes how the comparisons were made. The key AOT comparison results are presented and discussed in Section 4; surface reflectance comparison results are given and explained in Section 5. A summary of this work, and directions of potential further study are given in Section 6.

2 Datasets

2.1 Sentinel-2

S2 data is recorded by filter radiometers (instruments that measure incident radiation in a narrow spectral band) on two EO satellites (S2A and S2B), measuring 13 spectral bands from 443 nm to 2194 nm. Both satellites are in the same Sun-synchronous orbit, phased by 180°, in order to provide a five day revisit frequency at the Equator [5]; the Sun-synchronous orbit means that the satellites always pass surface positions at the same local time, giving consistency to observations. The S2 satellites provide high resolution measurements, at 10, 20, or 60 m resolution depending on the spectral channel, meaning that BOA reflectance values derived from S2 observations are desirable as an improvement to, for example, the lower resolution MODIS data. Data is provided in 'tiles' which are 110 km by 110 km regions of a UTM/WGS84 projection, which preserves angles and shapes but distorts area.

2.2 MODIS

MODIS is a filter radiometer currently in orbit on two sun-synchronous satellites, Aqua and Terra, which have different orbital paths and between them image the whole Earth every 1-2 days [6]. Data is obtained across 36 spectral bands ranging from 413 nm to 14.2 µm; land properties are typically investigated using 7 bands covering 469 nm to 2130 nm. MODIS data has been verified through multiple studies to agree with ground measurements, so can be assumed to give accurate results [7, 8, 9, 10]. Data are available in multiple different forms, of interest here is the Bidirectional Reflectance Distribution Function (BRDF) product (MCD43A1)[1], which describes surface reflectance as a function of incoming and outgoing radiation directions (the solar and view angles respectively). MCD43A1 data is produced in 1200 km by 1200 km tiles, using a sinusoidal projection, with a 500 m resolution.

2.3 AERONET

AERONET detectors are ground-based sun photometers that provide accurate measurements of AOT[2]. The measurements are available in three quality control levels, of which the highest quality is used here to provide the most reliable data, with a measurement error of 0.01 assumed on all AERONET AOT readings [11]. Detectors are randomly distributed worldwide; for this study sites were selected based on the land use and homogeneity of surrounding surface cover and the availability of AERONET data. The surface type was assessed using the Copernicus Land Monitoring Service's Global Land Cover map[3] and Table 1 details the chosen AERONET detectors. Case studies 1 and 2 have detectors located in forested areas in the Amazon and Pacific Northwest respectively. Case study 1 is surrounded by forest to beyond 50 km whilst Case study 2 is within roughly 20 km of farmland and urban areas. The detectors for Case studies 3 (Mongolia) and 4 (Israel) are both located within small urban areas but are largely surrounded by arid desert with little vegetation. Case study 5 is located near central Beijing, with a 10 km wide strip of forest at around 20 km from the detector.

AERONET measurements are made at wavelengths of 340, 380, 440, 500, 675, 870, 1020, and 1640 nm (meaning the detectors determine the optical path, caused by aerosols, at these wavelengths), whilst SIAC solves the AOT at 550 nm. Following Kaufman [12], a second order polynomial is fitted to log-transformed AERONET data, allowing interpolation to AOT at 550 nm, giving a direct comparison with SIAC AOT data.

[1]https://lpdaac.usgs.gov/products/mcd43a1v061/
[2]https://aeronet.gsfc.nasa.gov/
[3]https://land.copernicus.eu/global/products/lc

	Surface Type	AERONET Detector	Latitude (°)	Longitude (°)	S2 Tile
Case study 1	Forest	Amazon ATTO Tower	−2.14	−59.00	21MTT
Case study 2	Forest	NEON_WREF	45.82	−121.95	10TER
Case study 3	Bare/Sparse vegetation (desert)	Dalanzadgad	43.58	104.42	48TVP
Case study 4	Bare/Sparse vegetation (desert)	Sede Boker	30.86	34.78	36RXV
Case study 5	Built-up (urban)	Beijing-CAMS	39.93	116.32	50TMK

Table 1: Selected AERONET detectors, the surrounding surface type, their coordinates, and corresponding Sentinel-2 tile

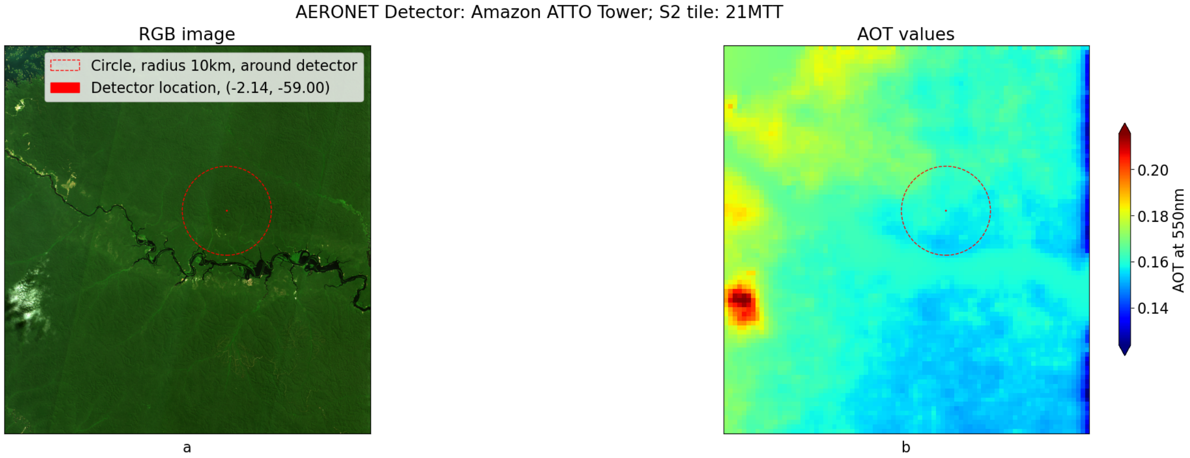

Figure 1: Plots of RGB (a), with bands at 665 nm, 560 nm and 490 nm, and AOT (b), measured at 550 nm, S2 data showing Case study 1, the Amazon ATTO Tower detector, location and a radius of 10 km around it, on 31/07/2020

3 Methodology

3.1 AOT comparison

After applying SIAC to S2 scenes for the relevant tiles, SIAC retrieved AOT values are compared with ground measurements from a variety of AERONET detectors. SIAC estimates AOT values at a 500 m spatial resolution, and its data should be averaged over multiple pixels to reduce random errors, whilst each AERONET detector makes measurements at a single stationary location, so the spatial variation of AOT needs to be considered. In studies comparing satellite-retrieved values with surface-measured values, satellite data is typically averaged across all 'clean' pixels within a predetermined distance from the ground detector. Previous work suggests that a radius of around 30 km is optimal for AOT comparison [13], therefore this work considers radii of this order: for each location SIAC pixel values are averaged within radii ranging from 1 km to 50 km in 1 km increments. For each radius a linear fit is calculated, representing the relationship between the SIAC averaged values and AERONET measurements across all S2 images of that Case study. The variation of root mean square error (RMSE) of the linear fit with radius is then considered in order to determine the optimum radius for AOT comparison for that Case study. At this radius the performance of SIAC is evaluated, with the optimal result being a one-to-one relationship between the SIAC-retrieved and AERONET-measured AOT values.

There is temporal variation between the SIAC and AERONET data, as SIAC provides measurements once every few days while AERONET records readings every 15 minutes (with occasional large gaps in the dataset). Following standard practice (as in [13]) for similar comparison work, AERONET readings within ±30 minutes of the S2 overpass are selected and averaged to compare to SIAC. A minimum of 3 AERONET readings in this time period is required, to reduce measurement errors.

As part of its processing, SIAC produces a cloud mask giving the probability of each pixel having cloud cover (at a 60 m resolution). In this work only scenes where more than 50 % of the pixels were cloud free are considered, where a cloud free pixel is defined as having less than a 20 % probability of being cloudy.

There is a generally accepted target that newly developed AC modules aim to achieve in their AOT retrievals: reaching a threshold uncertainty value of $\delta_{AOT} = 0.05 + 0.15AOT$ [3]. For SIAC to meet this threshold, 68 % of its AOT retrieval values should lie within this range centered on the reference (AERONET) values.

For the purposes of this work, bias is defined as

$$B = \frac{1}{n}\sum_{i=1}^{i=n} x_{SIAC} - x_{ref} \quad , \tag{1}$$

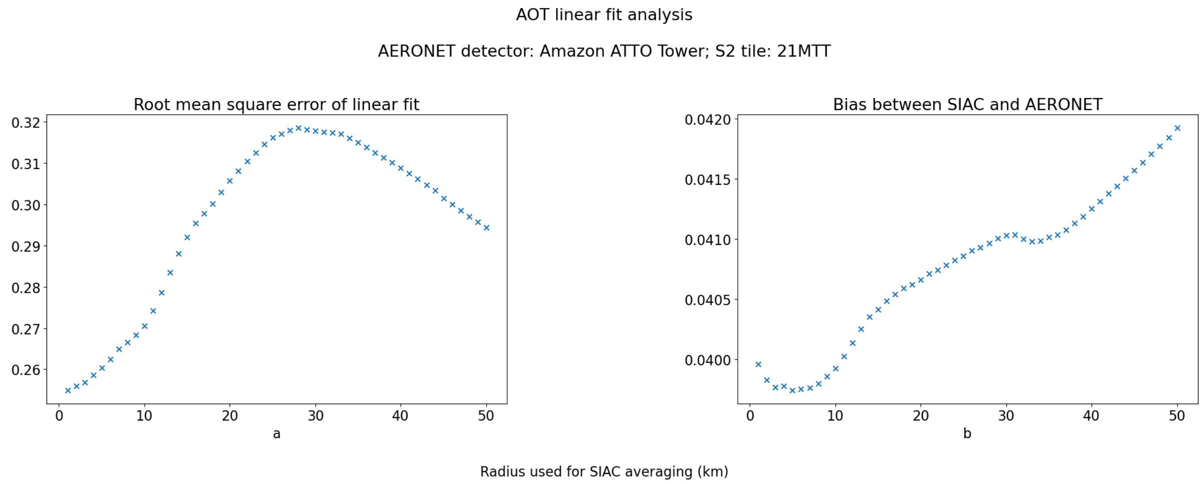

Figure 2: Linear ODR fit RMSE (a) and SIAC bias (b) as a function of the radius used for SIAC averaging, for Case study 1, the Amazon ATTO Tower detector. Using data from 39 images from 27/06/2016 to 13/12/2020

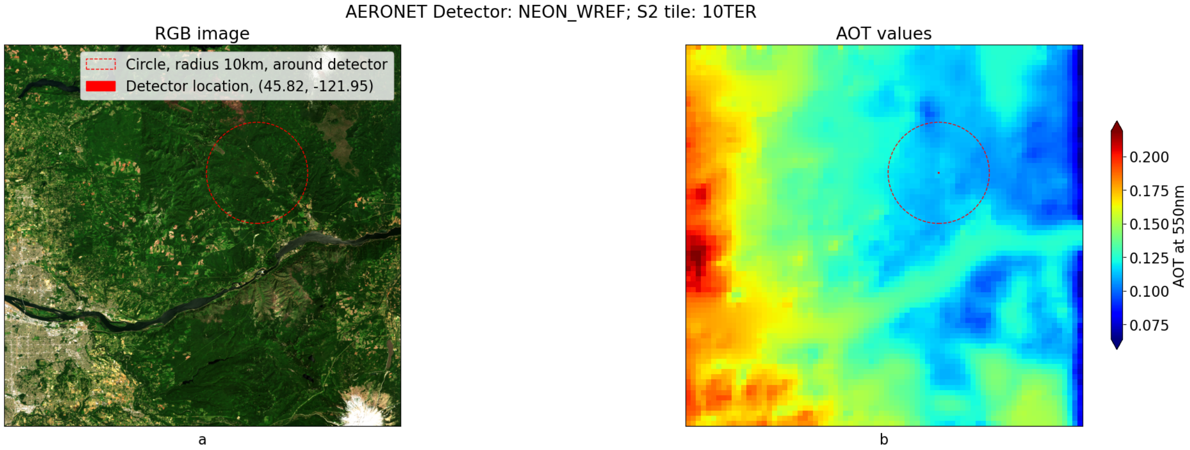

Figure 3: RGB (a) and AOT (b) plots from S2 data for Case study 2, the NEON_WREF detector, on 21/06/2021

where n is the number of images analysed, and x_{SIAC} and x_{ref} are the values retrieved by SIAC and the reference dataset of the required quantity.

3.2 Surface reflectance comparison

SIAC retrieved surface reflectance values in red, green and blue (RGB) visible bands, centered on 665 nm, 560 nm, and 490 nm respectively, were compared with equivalent values derived from the MODIS BRDF product, which has RGB bands centered on 645 nm, 555 nm, and 469 nm. Typically, different satellites make observations at different view angles (characterised by the azimuthal and zenith angles of the satellite relative to the scene) so inter-comparisons of this kind need to account for the effects of different viewing geometries. S2 satellite instruments make measurements at a single view angle, whereas MODIS collates measurements over 16 days, incorporating multiple angles and enabling the calculation of the BRDF. The two instruments also have different overpass times, resulting in distinct solar angles on the scene, which impacts the observed surface reflectance. Through its BRDF product, MODIS provides the parameters necessary to determine surface reflectance at any view and solar angles, so this can be used to derive an S2-equivalent MODIS retrieved reflectance value. The equations for this conversion are given in work by Roujean et al. [14], and the solar and view angles are taken directly from the SIAC output of the S2 data. The S2-equivalent MODIS values can then be compared with the SIAC values, using a time-series to allow comparison of non-simultaneous measurements. Where MODIS data is available and S2 data is not, linear interpolation is used to approximate solar and view angles of the S2 satellites. The comparison is made for a 3 by 3 grid of homogeneous MODIS pixels (1.5 km by 1.5 km), with SIAC data translated from S2's UTM/WGS84 projection to MODIS's sinusoidal projection. SIAC translated pixels are required to have less than a 5 % probability of cloud cover (a more rigorous condition is used than in AOT comparisons as cloud has a more significant impact on surface reflectance), whilst the 16 day averaging of the MODIS data mitigates the influences of clouds. The target uncertainty threshold for surface reflectance retrievals is $\delta_r = 0.005 + 0.05r$, where r is the BOA surface reflectance value.

4 AOT Comparison

4.1 Results: determining comparison radii

4.1.1 Case study 1: forest

Figure 1a shows an RGB image of the location of the Case study 1 AERONET detector, with its homogeneous forested surroundings. The AOT plot in Figure 1b illustrates the variation of AOT over the same spatial area as the RGB image, which appears relatively uniform. However, the river running from west to east has been un-

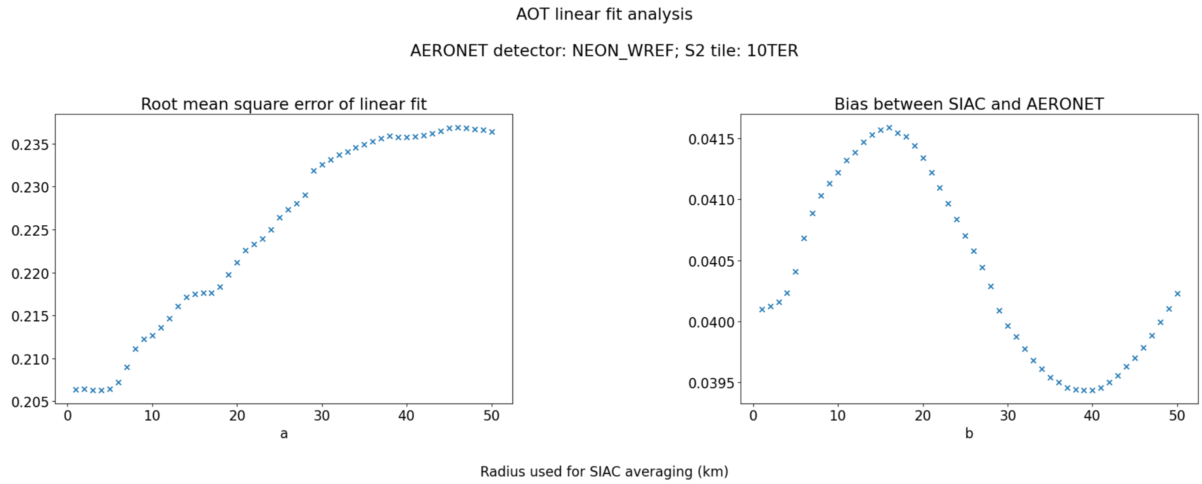

Figure 4: Linear ODR fit RMSE (a) and SIAC bias (b) as a function of radius averaging, for Case study 2, the NEON_WREF detector. Using data from 60 images from 12/02/2018 to 04/06/2021

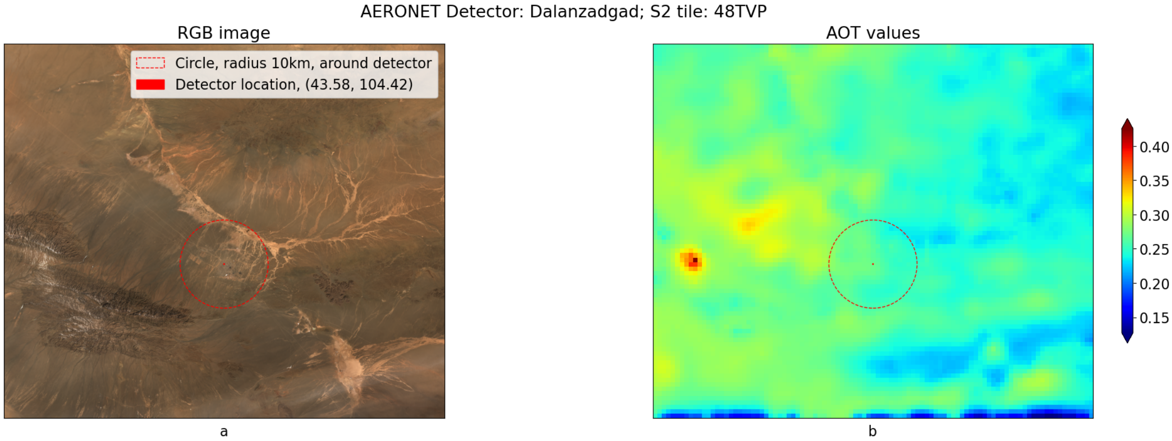

Figure 5: RGB (a) and AOT (b) plots from S2 data for Case study 3, the Dalanzadgad detector, on 19/03/2021

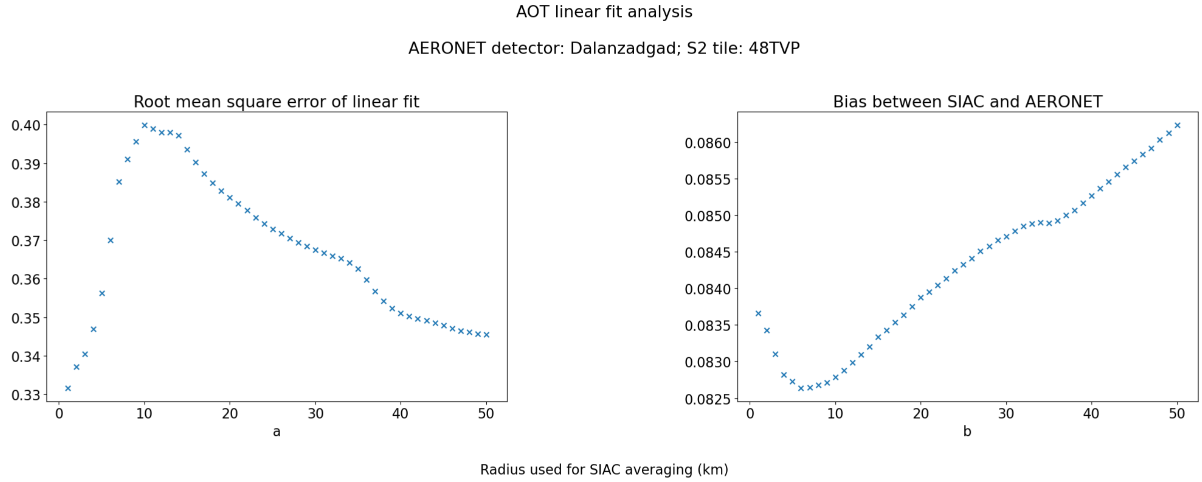

Figure 6: Linear ODR fit RMSE (a) and SIAC bias (b) as a function of radius averaging, for Case study 3, the Dalanzadgad detector. Using data from 166 images from 15/08/2015 to 28/08/2020

intentionally detected in the AOT retrieval as a band of higher values. There are also 'edge effects' on the right hand side of the S2 image; these commonly occur in satellite imagery. A comparison between the linear fitting of SIAC against AERONET data at different radii is given in Figure 2. The linear fitting method used is an Orthogonal Distance Regression (ODR)[4], considering errors in the y axis (SIAC) and x axis (AERONET). Despite the AERONET values being treated as reference values, they have measurement errors and variations between measurements made at different times, so cannot be considered to be 'true' values, making the standard least squares regression method inapplicable. Figure 2a shows that the RMSE between the measured and predicted SIAC values increases until a radius of 28 km, before decreasing again. SIAC is found to have a positive bias compared to AERONET values, with the bias increasing with radius. Considering these two parameters, a 10 km radius was used for the AOT comparison, as this has a lower RMSE than any larger radius. Radii under 10 km are not considered as these have larger uncertainties due to using fewer pixels in calculating the SIAC value.

4.1.2 Case study 2: forest

Figure 3 shows the expected increase of AOT towards the urban area on the western side of the tile, whilst edge ef-

[4]https://docs.scipy.org/doc/scipy/reference/odr.html

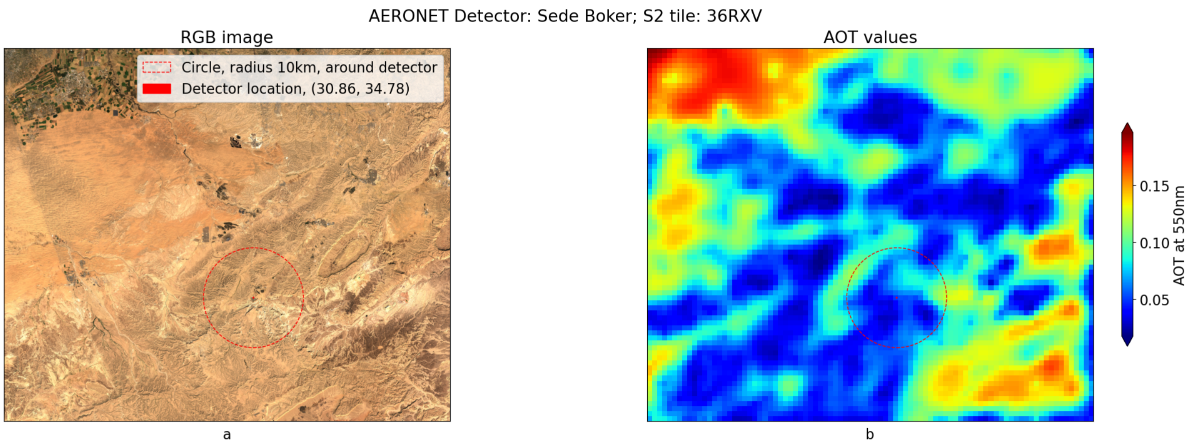

Figure 7: RGB (a) and AOT (b) plots from S2 data for Case study 4, the Sede Boker detector on 05/02/2020

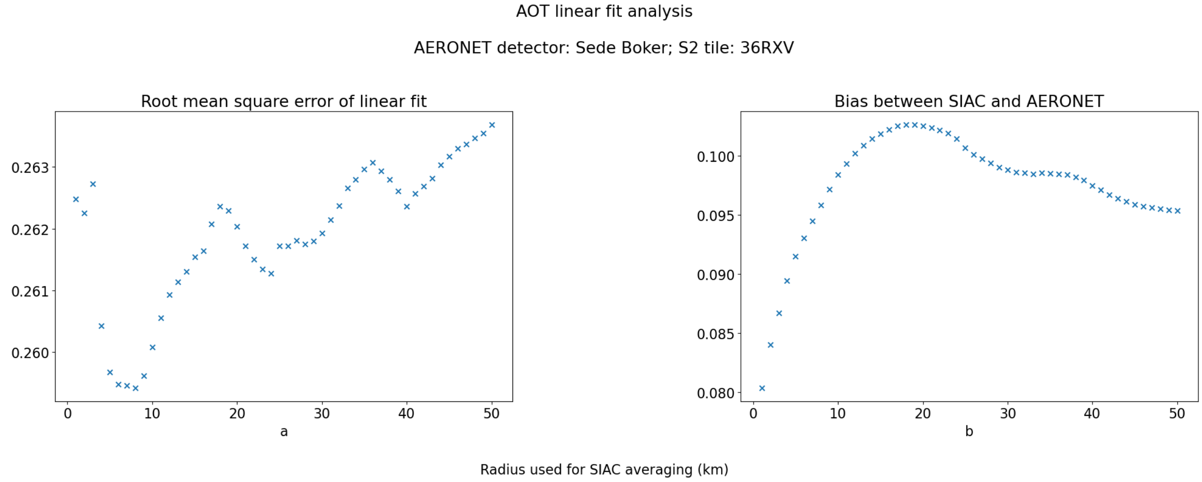

Figure 8: Linear ODR fit RMSE (a) and SIAC bias (b) as a function of radius averaging, for Case study 4, the Sede Boker detector. Using data from 68 images from 04/01/2017 to 05/02/2020

fects are again visible on the eastern edge of the scene. Figure 4a shows that RMSE increases as the comparison radius increases, so a radius of 10 km is again used. Figure 4b shows a decrease in bias at larger radii; this variation is likely due to the inhomogeneous AOT distribution and particularly the strong edge effects.

4.1.3 Case study 3: desert

The detector location is illustrated in Figure 5, showing uniform surface cover and fairly uniform AOT values. Figure 6a shows that the lowest RMSE is found at the largest radii, and so a comparison is made at 50 km.

4.1.4 Case study 4: desert

Figure 7 shows the other selected desert detector, with visibly higher AOT near the urban area in the northwest of the image, but fairly consistent values elsewhere. The performance comparison at varying radii is shown in Figure 8, with this another location where 10 km is the optimal comparison radius based on RMSE trends.

4.1.5 Case study 5: built-up

The location of the final Case study site is depicted in Figure 9; again this location shows, as expected, significantly higher AOT values over the urban area than the forested area. We can see that this location is inhomogeneous both at a large scale, with urban and forested regions, and at a small scale, with factories, parks and residential areas all being present in the urban regions. Looking at Figure 10a, the lowest RMSE is found at larger radii, so a comparison is made at 50 km. The decreased RMSE at larger radii suggests that the reduction in random error when considering a larger area has a more significant effect on the SIAC averaged result than the increase in AOT variation does.

4.2 Results: AOT retrieval validation

4.2.1 Case studies 1 and 2: forest

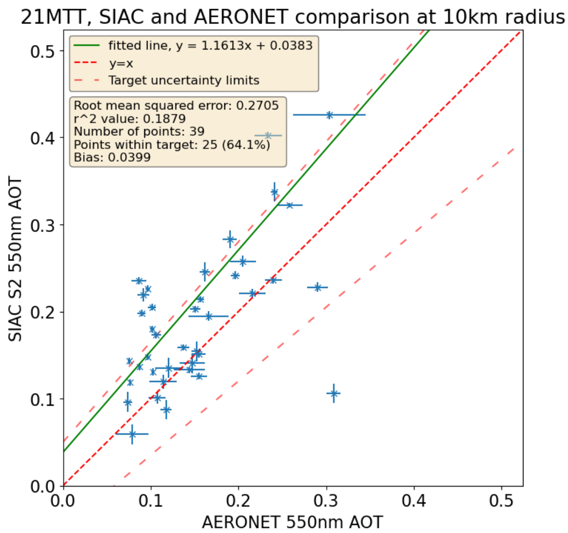

Figure 11: Scatter plot of SIAC and AERONET measured AOT values, showing a perfect 1 to 1 relation, target uncertainty bounds, and the calculated ODR linear fit, for Case study 1, the Amazon ATTO Tower detector. Data from 27/06/2016 to 13/12/2020

For Case study 1, the AOT comparison in Figure 11 shows a reasonable agreement between SIAC and

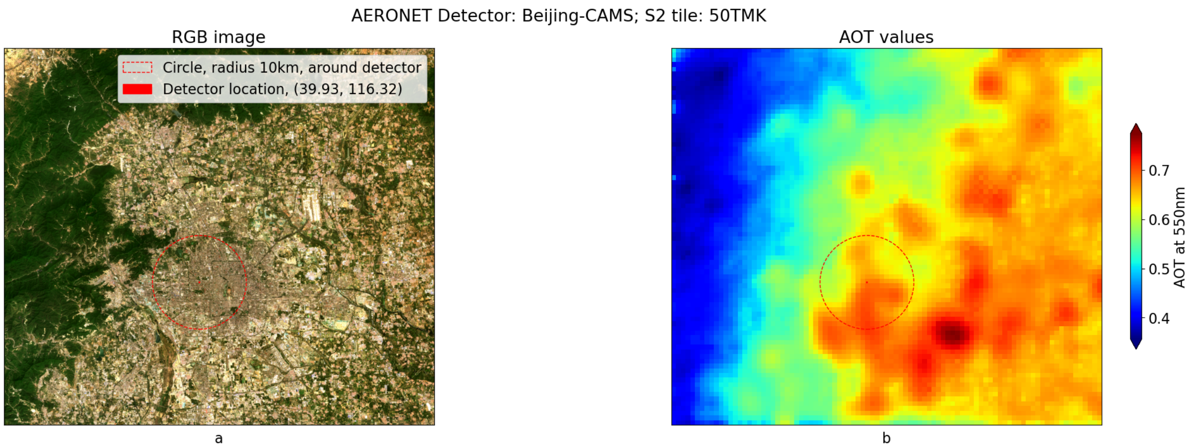

Figure 9: RGB (a) and AOT (b) plots from S2 data for Case study 5, the Beijing-CAMS detector on 23/05/2018

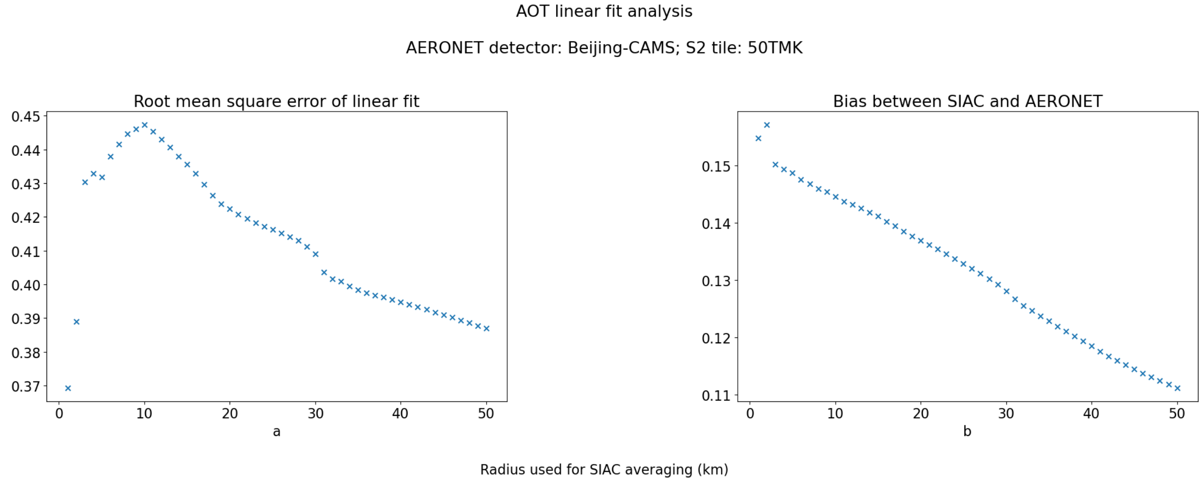

Figure 10: Linear ODR fit RMSE (a) and SIAC bias (b) as a function of radius averaging, for Case study 5, the Beijing-CAMS detector. Using data from 104 images from 27/02/2017 to 12/05/2020

AERONET values. The positive bias is quantified in a positive intercept and gradient larger than 1, however a high proportion (64.1 %) of the points lie within target uncertainty values as specified in Section 3.1. This is below the target value of 68 % but is an encouraging result given the relatively small sample size.

Figure 12 visualises the overall SIAC overestimation for Case study 2, with similar gradient and intercept values to Case study 1. Here 71.7 % of points lie within the uncertainty targets, which is a very strong result.

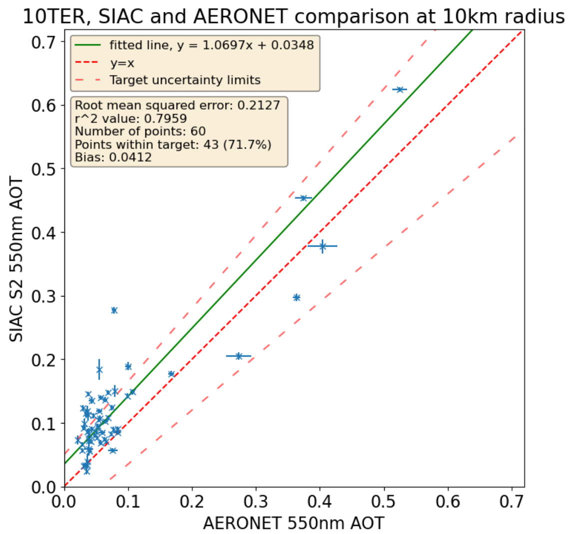

Figure 12: AOT comparison scatter plot for Case study 2, the NEON_WREF detector. Data from 12/02/2018 to 04/06/2021

4.2.2 Case studies 3 and 4: desert

The scatter plot at 50 km for Case study 3 is given in Figure 13, showing significantly worse SIAC performance than the two forest Case studies (1 and 2). Whilst the intercept is similar, the gradient is much larger and SIAC overestimation is clearer on the scatter plot with a larger bias. Only 45.2 % of points lie within target uncertainties.

At 10 km, the comparison for Case study 4 is made in Figure 14. This, as with the other desert Case study, provides compelling evidence of SIAC overestimation, characterized by a large intercept and a low percentage (30.9 %) of points within the uncertainty bounds. The remaining 69.1 % of points all demonstrate SIAC overestimation.

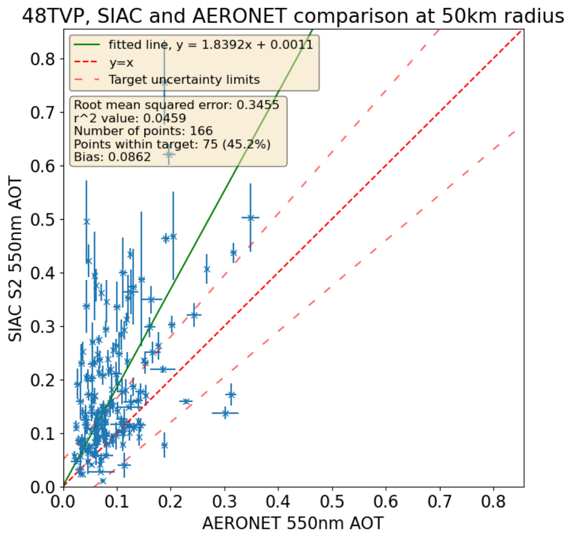

Figure 13: AOT comparison scatter plot for Case study 3, the Dalanzadgad detector. Data from 15/08/2015 to 28/08/2020

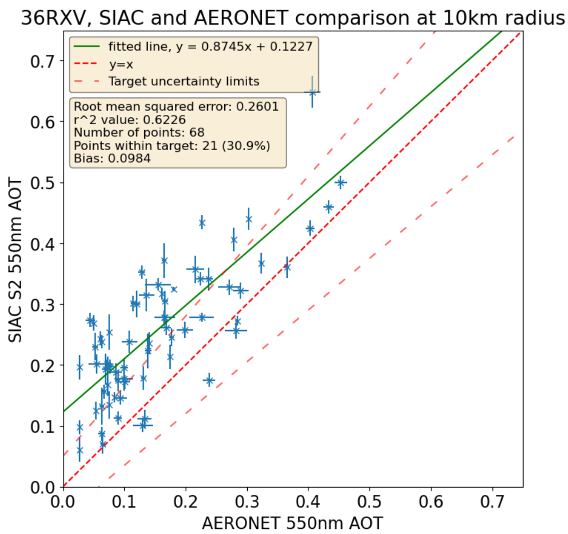

Figure 14: AOT comparison scatter plot for Case study 4, the Sede Boker detector. Data from 04/01/2017 to 05/02/2020

4.2.3 Case study 5: built-up

Figure 15 for Case study 5 shows similar results to Case studies 1, 2, 3 and 4 with a general overestimation by SIAC resulting in a positive intercept and gradient larger than 1; it has a low percentage of points within the target uncertainty values at only 32.7 %. This is significantly lower than both of the forest sites (Case studies 1 and 2).

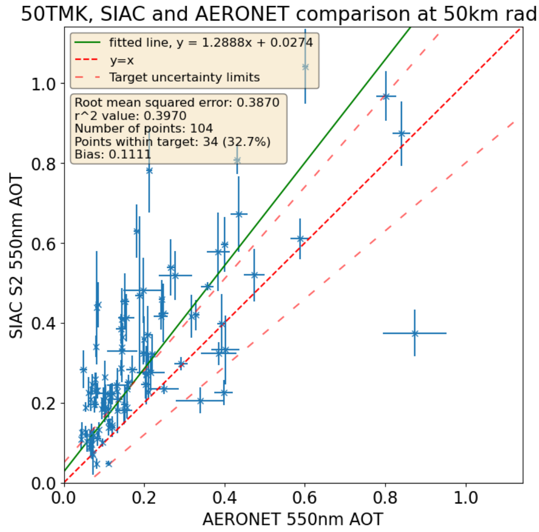

Figure 15: AOT comparison scatter plot for Case study 5, the Beijing-CAMS detector. Data from 27/02/2017 to 12/05/2020

4.3 Discussion

There is a clear trend across all five analysed locations for SIAC overestimating the AOT. Each location shows a positive intercept and most a gradient larger than 1, so the bias increases as the AOT value increases. Performance is good in the forest sites (Case studies 1 and 2, Figures 11 and 12), with an average of 67.9 % of points within the target uncertainty bounds, and an average bias of 0.0406. Over the desert sites (Case studies 3 and 4, Figures 13 and 14), performance is significantly worse with 38.1 % of points within the target bounds and a bias of 0.0923. This degradation of performance over brighter surfaces is not unexpected for an aerosol retrieval: light reflected from the surface represents noise whilst light scattered from the aerosols is the signal, so if the surface reflectance is higher then the signal to noise ratio is lower and AOT retrievals typically give worse results [15]. However, the decreased signal to noise ratio should only increase the uncertainty in SIAC's AOT retrievals and not the bias, and so comparing the results between forest and desert Case studies shows that SIAC's AOT retrieval is significantly worse over the desert sites. The desert sites have 29.9 % fewer points within target uncertainties, and a bias that is over 2 times larger than that of the forest sites.

Case study 5 (the urban region) also shows poor results with 32.6 % of points within target uncertainties and a bias of 0.1111. This is the highest bias of any of the locations and suggests SIAC's AOT retrievals are less accurate over urban areas than over deserts or forests. As previously discussed in Section 4.1.5, this site shows large-scale inhomogeneity and this may be affecting the results. The AOT is less uniform across the urban area than in other Case studies, so averaging SIAC across a wide region is not representing the SIAC retrieval at the AERONET detector location. This will always be a challenge when analysing SIAC AOT performance over urban areas using this method, as very few urban areas cover a 50 km radius around an AERONET detector with uniform AOT within that region. It is also possible that the small-scale inhomogeneity of Case study 5 is decreasing the accuracy of the SIAC results: because the characteristic size of surface use in this region, such as buildings and urban parks, is larger than the high resolution S2 pixels and smaller than the lower resolution MODIS pixels, SIAC's method of projecting S2 data onto a 500 m resolution to match MODIS may introduce larger errors than for more homogeneous areas. This is an inherent shortcoming of SIAC's method and suggests that its AOT retrievals over areas with small-scale inhomogeneities will always be less accurate than over more homogeneous regions. This Case study also includes higher values of AOT than the other Case studies, however there is inconclusive evidence of inconsistent SIAC retrieval for higher AOT values due to a lack of very high AOT values.

Visually comparing the AOT images to the RGB images (Figures 1, 3, 5, 7 and 9) also provides some insights into SIAC's performance, despite each image only representing one observation of the scene. The patterns of AOT agree with expectations of higher values over urban areas which qualitatively supports good performance by SIAC, albeit at a rather basic level. It is also of interest that the AOT retrieval has picked up the patterns of the rivers in tiles 21MTT and 10TER (Figures 1 and 3 respectively). There is no physical reason for the true AOT values to be any different above the rivers, so this represents a shortcoming in SIAC's AC method. The likely source is the MODIS BRDF data which has varying accuracy across different surface types, with this inconsistency being maintained through the SIAC AOT retrieval to give an optimal estimate with an AOT that is noticeably different above the rivers. This highlights an unavoidable issue with SIAC in that it relies on MODIS BRDF data being correct, and any error in MODIS data will be propagated through to SIAC processed data.

5 Surface reflectance Comparison

5.1 Results

A comparison time series for a homogeneous region in the Case study 1 (forest) tile is shown in Figure 16. This demonstrates that SIAC performs moderately well in comparison to the MODIS data with the seasonal trends matching, such as the increase in surface reflectance in the summer of 2018. None of the analysed bands show SIAC reaching performance targets as specified in Section 3.2, with an overall average of 50 % of points within the target uncertainty bounds. However, the calculated statistics are not fully representative of SIAC's accuracy, as they are derived from an inter-comparison of satellite data rather than a validation with ground measurements. Consequently, these calculations are limited by inaccuracies in the reference dataset, here the MODIS BRDF data. The red and green bands both show SIAC underestimating surface reflectance with biases of −0.0066 and −0.0061 respectively, whilst the blue band shows SIAC overestimating the surface reflectance with a bias of 0.0010.

A homogeneous desert region in the Case study 3 tile

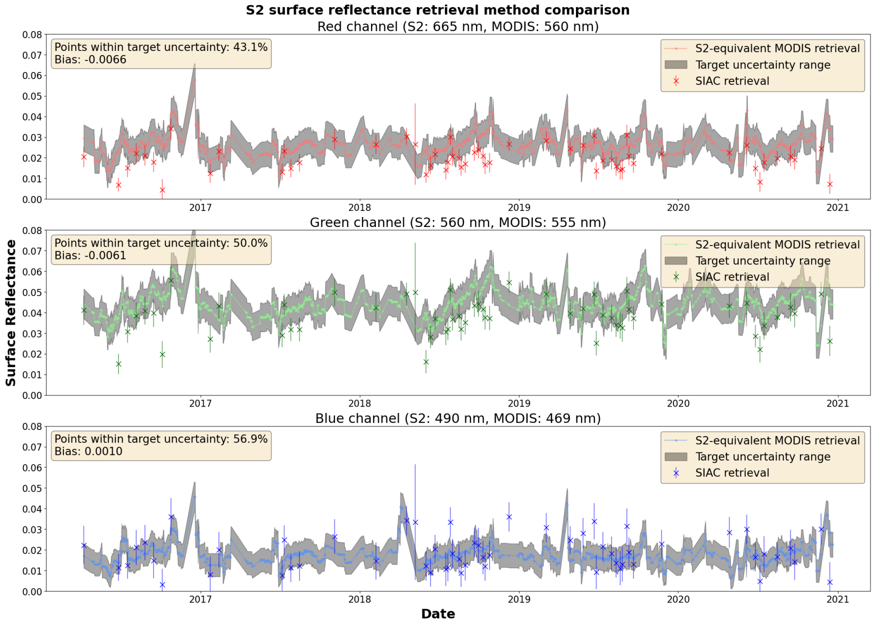

Figure 16: A time series from 08/04/2016 to 13/12/2020 of SIAC and MODIS retrieved surface reflectance in S2 viewing geometry for the red, green, and blue visible bands over a region of the S2 tile for Case study 1

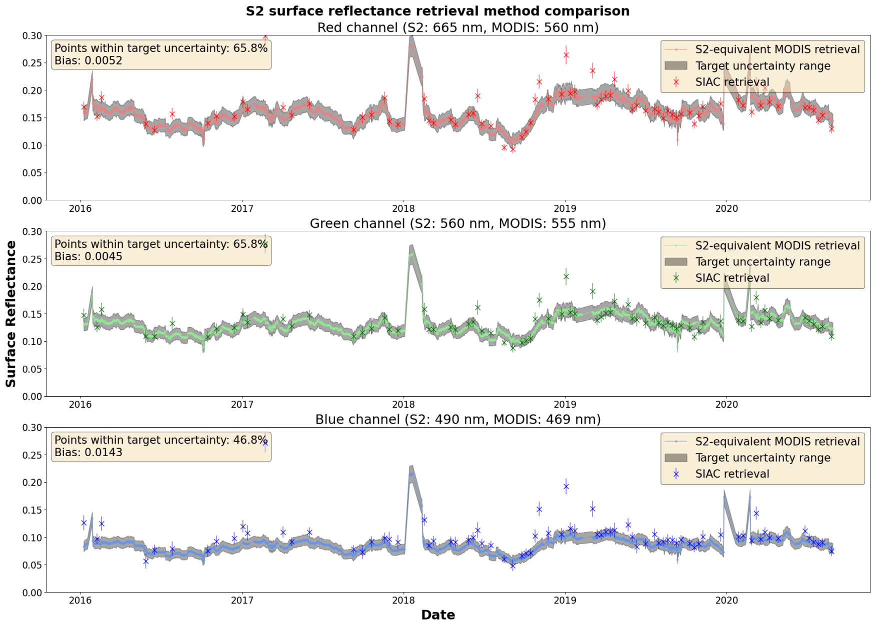

Figure 17: A time series from 09/01/2016 to 25/08/2020 of surface reflectance data over a region of the S2 tile for Case study 3

is also analysed, with the results shown in Figure 17. This indicates similar results to the comparison in the Case study 1 tile, with SIAC matching the trends in MODIS data, although here we have closer agreement and more SIAC points within the target uncertainties, an average of 59.5 %. The comparison in the Case study 3 tile shows SIAC overestimation for all three bands, with the largest overestimation occurring in the blue band, which has a bias of 0.0143 whilst bias in the red band is 0.0052 and the green band bias is 0.0045. This is a similar trend to the Case study 1 comparison (Figure 16) where the blue band has a more positive bias than either of the red and green bands.

5.2 Discussion

The surface reflectance comparison shows largely encouraging results, with SIAC able to identify the major trends in surface reflectance (as observed by MODIS), and also detect some of the shorter term variability. It can be seen that SIAC overestimates surface reflectance for the desert site (Case study 3, Figure 17) giving a mean bias of 0.008 across the three bands, whilst it makes an underestimation for the forest site (Case study 1, Figure 16) with a mean bias of -0.004. This contrasts with the AOT results which SIAC overestimated on both surface types, with a larger positive bias over desert sites (0.0923 on desert sites and 0.0406 on forest sites). This suggests that SIAC's general performance on surface reflectance is likely more accurate than its AOT retrieval due to biases across different surface types being distributed around zero, rather than all being positive. For any given location (excluding snowy scenes), the surface brightness is likely to lie between that of the forest and desert sites. Therefore assuming that the AOT retrieval bias is positively correlated to the surface brightness, as seems to be the case here, the AOT overestimation will be bounded by that found for forest and desert sites (biases of 0.0406 and 0.0923 respectively). Similarly, the surface reflectance bias is likely bounded by the overestimation found for the desert scene (bias of 0.008) and the underestimation present in the forest scene (bias of -0.004). This means the SIAC retrieved surface reflectance will be closer to MODIS BRDF derived results than the SIAC retrieved AOT value is to AERONET measurements.

However, there are shortcomings in the quantitative results obtained here. Firstly, the comparison method is only an inter-comparison between satellite data, not a validation of SIAC results compared to more accurate ground measurements. This introduces larger uncertainty and potential bias in the 'reference' data. Secondly, the spectral bands of the different filter radiometers are not exactly matched, so different measurements of identical scenes are to be expected. Nonetheless, these initial results are encouraging, and point towards SIAC providing an accurate high resolution surface reflectance product.

6 Conclusion

AC modules derive BOA results from TOA satellite measurements by accounting for atmospheric scattering and absorption by aerosols and water vapour. The SIAC module aims to provide atmospheric corrections for the S2 and L8 satellites through a Bayesian framework, in order to produce high resolution surface reflectance data. 437 S2 scenes across five different locations are processed with SIAC, matched spatially and temporally to AERONET measurements and analysed to determine the accuracy of the SIAC AOT retrievals. Surface reflectance data from S2 scenes of a forest location and a desert location are compared with MODIS surface reflectance data across a four year time period.

SIAC AOT results are found to be variable across different surface types, with good accuracy in forested areas (67.9 % of points within target uncertainties and a bias of 0.0406) but worse results in deserts (38.1 % of points within target uncertainties and a bias of 0.0923) and an urban area (32.6 % of points within target uncertainties and a bias of 0.1111). Further analysis of other sites with small-scale land use inhomogeneities is required to determine if the poor AOT retrieval at the urban location is due to signal to noise effects, unavoidable issues with the validation method when applied to areas with large-scale inhomogeneity such as is the case here, or a more inherent issue with SIAC with the small-scale inhomogeneity being observed differently by S2 and MODIS.

SIAC surface reflectance results are analysed for a region of forest and a region of desert. Results are encouraging in both cases, showing general agreement with seasonal trends in MODIS data with biases of -0.004 and 0.008 respectively. None of the analysed bands achieve the target uncertainty limits, however the inter-comparison method limits the best possible result. Further investigation is recommended, including comparison of surface reflectance results across a wider variety of surfaces, a more thorough validation utilising ground measurements (for example from RadCalNet detectors), and improved accuracy in the inter-comparison method by accounting for different spectral response functions of the S2 and MODIS filter radiometers.

References

[1] S. Liang and J. Wang. "Advanced Remote Sensing (Second Edition)". In: Academic Press, 2020. Chap. 4 - Atmospheric correction of optical imagery, pp. 131–156. ISBN: 9780128158265.

[2] F. Yin et al. "Bayesian atmospheric correction over land: Sentinel-2/MSI andLandsat 8/OLI". In: *Geoscientific model development* (2022).

[3] G. Doxani et al. "Atmospheric Correction Inter-comparison eXercise, ACIX-II Land: An assessment of atmospheric correction processors for Landsat 8 and Sentinel-2 over land". In: *Remote Sensing of Environment* (2023).

[4] Y. Li et al. "Evaluation of Sentinel-2A Surface Reflectance Derived Using Sen2Cor in North America". In: *IEEE Journal of Selected Topics in Applied Earth Observations and Remote Sensing* (2018).

[5] URL: `https://sentinels.copernicus.eu/web/sentinel/missions/sentinel-2/data-products`.

[6] URL: `https://modis.gsfc.nasa.gov/about/`.

[7] S. Liang et al. "Validating MODIS land surface reflectance and albedo products: methods and preliminary results". In: *Remote Sensing of Environment* (2002).

[8] J. Liu et al. "Validation of Moderate Resolution Imaging Spectroradiometer (MODIS) albedo retrieval algorithm: Dependence of albedo on solar zenith angle". In: *Journal of Geophysical Research* (2009).

[9] A. Roesch, C. Schaaf, and F. Gao. "Use of Moderate-Resolution Imaging Spectroradiometer bidirectional reflectance distribution function products to enhance simulated surface albedos". In: *Journal of Geophysical Research* (2004).

[10] X. Che et al. "Assessment of MODIS BRDF/Albedo Model Parameters (MCD43A1 Collection 6) for Directional Reflectance Retrieval". In: *Remote Sensing* (2017).

[11] D. M. Giles et al. "Advancements in the Aerosol Robotic Network (AERONET) Version 3 database – automated near-real-time quality control algorithm with improved cloud screening for Sun photometer aerosol optical depth (AOD) measurements". In: *Atmospheric Measurement Techniques* (2019).

[12] Yoram J. Kaufman. "Aerosol optical thickness and atmospheric path radiance". In: *Journal of Geophysical Research: Atmospheres* (1993).

[13] C. Ichoku et al. "A spatio-temporal approach for global validation and analysis of MODIS aerosol products". In: *Geophysical Research Letters* (2002).

[14] J. L. Roujean, M. Leroy, and P. Y. Deschamps. "A Bidirectional Reflectance Model of the Earth's Surface for the Correction of Remote Sensing Data". In: *Journal of Geophysical Research* (1992).

[15] Yoram J. Kaufman. "Satellite Sensing of Aerosol Absorption". In: *Journal of Geophysical Research* (1987).